

Electrochemical Techniques for the Characterization of Redox Polymers

Adrian W. Bott, Ph.D.

Bioanalytical Systems, Inc.
2701 Kent Avenue
West Lafayette, IN
47906-1382

Email:
awb@bioanalytical.com

This article discusses the different electroanalytical techniques that have been used to characterize redox polymers immobilized on electrode surfaces.

One of the most intensively studied areas in electroanalytical chemistry for the past two decades has been modification of electrode properties by the immobilization of redox-active species onto the electrode surface by their incorporation into a polymer (1-3). For example, one common application has been the immobilization of enzymes (together with mediators) for the electrochemical detection of biologically important species (e.g., glucose) (4). This article will discuss the electrochemical techniques that are used to characterize these redox polymers.

It is important at this stage to differentiate between redox polymers and conducting polymers. Redox polymers contain spatially and electronically localized redox sites. These can be either covalently bound to the polymer (e.g., polyvinyl-pyridine or polymerized metal bipyridine complexes) or electrostatically bound (e.g., negatively charged metal chloride or cyanide

complexes in protonated poly [vinylpyridine] or positively charged metal bipyridine complexes in Nafion). In contrast, conducting polymers (which will not be discussed in this article) contain delocalized electronic states.

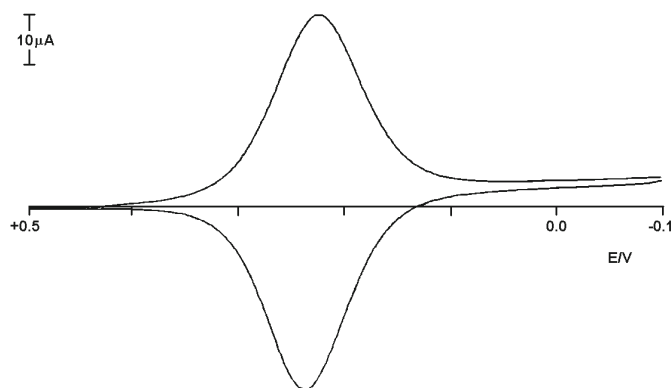
The current response of redox polymer films depends upon the relative sizes of the diffusion layer δ (the layer adjacent to the electrode surface where the concentrations differ from those in the bulk polymer) and the film thickness ϕ . There are two limiting cases to consider—semi-infinite diffusion ($\phi \gg \delta$) and thin-layer behavior ($\phi \ll \delta$). The current responses for semi-infinite diffusion are well-known from studies of solution redox species, although the mechanism for diffusion in polymer films is different (*vide infra*), and the diffusion coefficients for polymer films generally a few orders of magnitude smaller than those for species in solution. In contrast, diffusion is not important for systems exhibiting thin layer behavior, since

the electroactive material immobilized on the electrode surface is electrolyzed very rapidly when the applied potential is changed.

Many redox polymers exhibit behavior that is intermediate between these two limiting cases. This behavior is referred to as finite diffusion. As discussed above, the important parameters in determining the extent of diffusion effects are the thickness of the diffusion layer δ and the film thickness ϕ . δ depends upon the diffusion coefficient (D) and the experimental time scale t_e . The effects of D , δ , and ϕ can all be expressed using the dimensionless variable Dt_e/ϕ^2 . If this is much larger than 1 (large D , a long experimental time scale, and/or a thin film), then thin layer behavior will be observed, whereas if it is much less than 1 (small D , a short experimental time scale, and/or a thick film), the system will exhibit semi-infinite behavior.

In redox polymer films, D is related to charge transfer through the polymer; for example, the rate of

Cyclic voltammogram for a ferrocyanide/polyvinylpyridine film at a scan rate of 20 mV s^{-1} . Reprinted from ref. 7 with permission from Elsevier Science.



electron transfer between the electrode surface and the redox centers (5). There are two possible mechanisms for this; physical motion of the redox centers, and electron transfer between adjacent oxidized and reduced redox centers (electron hopping). This is in contrast with diffusion in dilute solutions, which is determined only by the physical motion of the redox-active molecules. The relative importance of these two mechanisms depends upon the system. For example, the pyridine-pentacyanoferrate complex can be either electrostatically-bound or covalently-bound to a poly(vinylpyridine) polymer, and it was found that D for the electrostatically-bound system was two orders of magnitude larger than for the covalently-bound system (6). This difference was attributed to the fact that both mechanisms are possible for electrostatically-bound redox centers, whereas physical motion is not possible for covalently bound centers (other than the limited movement allowed by segmental polymer motion), and only the electron hopping mechanism is possible.

Since electron transfer reactions of redox polymers must be accompanied by counterion exchange between the polymer and the solution (in order to maintain electroneutrality), it is conceivable that movement of these counterions within the polymer film may be the current limiting factor. However, it has been observed that this movement is much faster than the rate of electron transfer, and hence has little effect on the

current response. The rapid rate of counterion diffusion precludes the formation of electric fields within the polymer film, and hence eliminates any migration effects.

Cyclic Voltammetry

Cyclic voltammograms of redox polymers are typically run at very slow scan rates (e.g., $5 - 10 \text{ mV s}^{-1}$) in order to observe thin-layer behavior (i.e., a long experimental time scale). The ideal cyclic voltammogram run under these conditions shows two symmetrical peaks, with a peak potential separation of 0 mV , and a half-peak width of 90.6 mV . The cyclic voltammogram of ferrocyanide immobilized in poly(vinylpyridine) exhibits close to ideal behavior (F1) (7). However, most redox polymers do not yield ideal voltammograms; in particular, the half-peak widths are generally larger than 90.6 mV . This has been attributed to repulsive interactions between the redox centers (8) and small variations in the local environments of different redox centers, giving rise to a range of redox potentials (2,3). Interactions between redox centers can be incorporated into the model for the layer by using the Temkin isotherm rather than the Langmuir isotherm; this introduces a parameter (g), which quantifies the extent of the interactions.

It is also important to note that, for thin layer systems, cyclic voltammetry is a coulometric experiments; that is, all the redox centers in the film are electrolyzed during the po-

tential scan. Therefore, based on Faraday's Law ($Q = nF\Gamma A$), the number of redox centers in a film (ΓA) (where Γ is the surface coverage in moles cm^{-2} and A is the electrode surface area in cm^2), and hence the charge storage capabilities of the film, can be calculated from the total charge passed (Q). The concentration of redox species C can then be calculated if the electrode surface area and film thickness ϕ (measured using e.g., ellipsometry and scanning electron microscopy) are known ($C = \Gamma A / A\phi = \Gamma / \phi$). However, it is important to note that the values of the film thickness obtained from these *ex situ* techniques may not accurately reflect the thickness of the film in the solution due to solvent exchange upon immersion in solution, and the solvent and counterion exchange that occurs as a result of the electron transfer reaction.

An alternative method for plotting a cyclic voltammogram is to plot i/v vs. E , where v is the scan rate. The quantity i/v is referred to as the *pseudo-capacitance* (or *redox capacitance*) ΔC of the film. Although the film is not strictly a capacitor (there is no separation of charge), the mathematical definition is similar to that of a capacitor. ΔC is an alternative parameter for expressing the number of redox centers in the polymer film (i.e., the ability of the film to store charge), and is related to Γ by the following equation:

$$\Delta C = \frac{n^2 F^2 \Gamma}{RT} \cdot f(1-f)$$

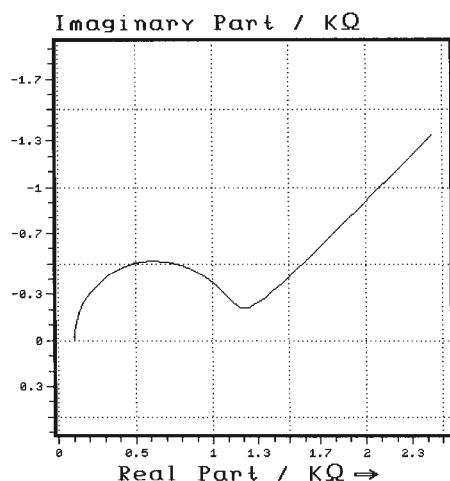
where f is the proportion of oxidized species [$C_O / (C_O + C_R)$]. ΔC therefore has its maximum value at $f = 0.5$ (i.e., at the redox potential).

Chronocoulometry

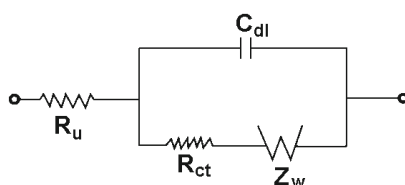
The application of chronocoulometry to the study of redox polymer films is based on the linear relationship between the charge and the square root of time (the Anson plot). This relationship requires semi-infinite diffusion, and hence the time scales of these experiments

F2

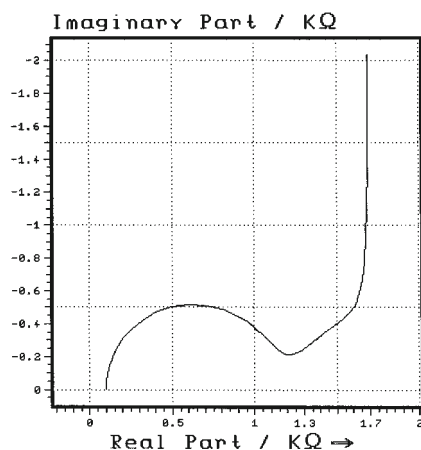
Idealized Nyquist plot for a redox active species in solution.

**F3**

Randles equivalent circuit for a redox active species in solution.

**F4**

Idealized Nyquist plot for a redox polymer film.



are short (typically less than one second). D can be calculated from the slope (S) of the Anson plot, based on the following equation:

$$D = \left(\frac{\pi}{4} \right) \left(\frac{S}{nFAC} \right)^2$$

where A is the electrode surface area, and C is the concentration of the redox centers in the film. It is often difficult to calculate C , since the film thickness must be known (*vide supra*).

Electrochemical Impedance Spectroscopy

Electrochemical impedance spectroscopy (EIS) is based on the perturbation of a system at equilibrium by a small amplitude AC potential wave form (typically 5 -10 mV). It is therefore fundamentally different from the two large amplitude techniques discussed above in that the perturbations to the system under study are small. Another advantage of EIS is that a range of different experimental time scales are examined within the one experiment by examining the impedance of the system over a range of frequencies. Fur-

thermore, the two parameters discussed above (Γ and D) can be measured in the same experiment.

A common approach for the interpretation of impedance spectra is the method of equivalent circuits (9), which states that the components of an electrochemical and mathematical cell can be modeled using electronic and theoretical components: that is, circuit can be built that has an impedance spectrum identical to that of the electrochemical system under investigation. There are two important criteria for identifying the correct equivalent circuit:

1. There must be a good match between the experimental impedance spectrum and the model impedance spectrum over the entire frequency range.
2. Each of the electronic components of the equivalent circuit must be related to one of the parameters of the experimental system.

As an example, let us consider the impedance spectrum (expressed as a Nyquist plot) for a redox-active species in solution (F2), which consists of a semi-circle at high frequencies, and a straight line at low frequencies. This system can be modeled using the Randles circuit (F3). The semi-circle at high frequencies is related to the parallel combination of the double-layer capacitance (C_{dl}) and the charge-transfer resistance (R_{ct}), whereas the straight line at an angle of 45° to the x axis at low frequencies is related to the Warburg diffusion parameter. In other words, at high frequencies (short time scales), the impedance is determined by slow electron transfer kinetics, whereas at lower frequencies (longer time scales), the impedance is diffusion-controlled. This is analogous to the variation of the current response with scan rate for cyclic voltammetry; that is, the current can be diffusion-controlled at slow scan rates (long time scales), but increasing the scan rate (shortening the time scale) can lead to limitations by

electron transfer kinetics. However, whereas multiple cyclic voltammetry experiments must be run to examine the effect of varying the experimental time scale, a range of different time scales can be examined in one EIS experiment.

As discussed above, one of the factors that determines whether thin layer behavior or semi-infinite diffusion is observed is the time scale. Since an EIS experiment has multiple time scales, both can be observed, and this is shown in an ideal Nyquist plot for a redox polymer (F4). At high frequencies, the impedance is again determined by electron transfer kinetics. Semi-infinite diffusion is observed when the wavelength of the AC potential is small relative to the film thickness (i.e.,

intermediate frequencies) and is again characterized by a straight line at an angle of 45° to the axis. However, when the AC wavelength is comparable with the film thickness (lower frequencies), the system is under thin layer conditions, which is characterized by a straight line perpendicular to the x axis.

The ideal impedance spectrum of a redox polymer film can be modeled using a modified Randles circuit (F5). The Warburg element for semi-infinite diffusion has been replaced by the diffusion element Z_D , which is defined by the following equation:

$$Z_D = \frac{A}{(j\omega)^{1/2}} \coth \left[B(j\omega)^{1/2} \right]$$

At large x , $\coth x = 1$, hence

$$Z_D = \frac{A}{(j\omega)^{1/2}}$$

which is a mathematical representation of the Warburg impedance (semi-infinite diffusion). At small x , $\coth x = 1/x + x/3$, hence

$$Z_D = \frac{A}{j\omega B} + \frac{AB}{3}$$

which corresponds to a series combination of a resistance of $AB/3$ and a capacitance B/A . The impedance spectrum of such a series combination is a straight line perpendicular to the x axis. For a polymer film, this resistance is the film resistance R_F , and the capacitance is the pseudo-capacitance ΔC discussed above (*vide supra*).

Therefore, the important parameters that can be extracted from the impedance spectrum of a redox polymer are the charge transfer resistance (R_{CT}), the Warburg coefficient (σ), the film resistance (R_F), and the film pseudo-capacitance (ΔC) (however, it should be noted that, depending upon the time scales of the various processes, not all these may affect a given impedance spectrum). For an ideal system, these parameters can be derived from equivalent circuits, or from specific analysis of certain data segments. For example, a plot of Z vs. $\omega^{-1/2}$ for the region of semi-infinite diffusion has a slope of σ (F6), and a plot of Z'' vs. ω^{-1} for the thin layer region has a slope of ΔC^{-1} (F7) (10).

Once these parameters have been extracted from the impedance spectrum, they can be used to calculate D using the relationships below.

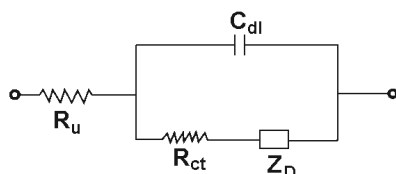
$$R_F \Delta C = \frac{B^2}{3} = \frac{1}{3} \left(\frac{\phi}{D^{1/2}} \right)^2$$

$$\sigma = \frac{1}{\Delta C \sqrt{2}} \cdot \left(\frac{\phi}{D^{1/2}} \right)$$

These calculations actually generate a value for $(\phi/D^{1/2})$, and other methods must be used to calculate or estimate ϕ . The ambiguities associated with such measurements (*vide supra*) limit the accuracy of the val-

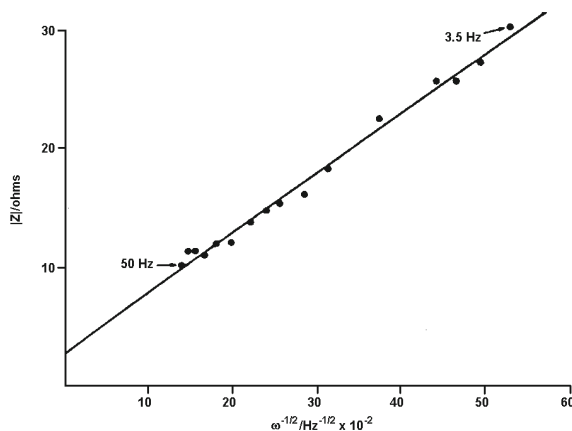
F5

Modified Randles circuit for a redox polymer film.



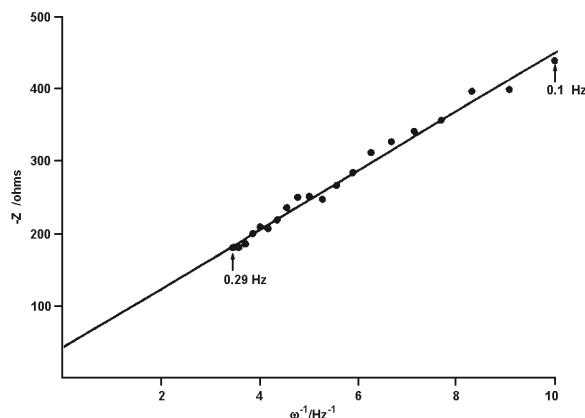
F6

Plot of Z versus $\omega^{-1/2}$ for a polyvinylferrocene film using data from the semi-infinite region of the spectrum. Reprinted from ref. 10.

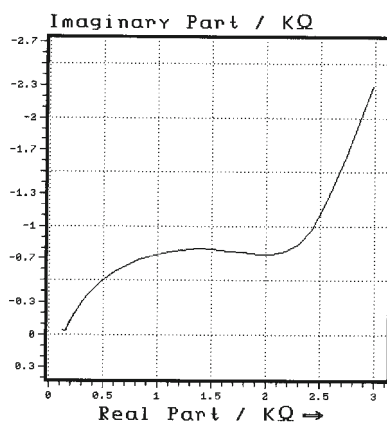


F7

Plot of Z'' versus ω^{-1} for a polyvinylferrocene film using data from the thin layer region of the spectrum. Reprinted from ref. 10.



Impedance spectrum for an osmium/polyimidazole polymer film.



ues of D obtained using impedance spectroscopy.

The ideal impedance spectrum shown in **F4** is rarely observed for real redox polymers. For real systems, the low frequency limit is typically a straight line at an angle of less than 90° with the x axis (in addition, the angle of the line in the semi-infinite region may be less than 45°), due to non-idealities in the finite boundary (**F8**) (11). This behavior can be modeled by replacing the finite diffusion (coth) element used for the ideal circuit by the elements that define the limiting cases; that is, a Warburg impedance (for semi-infinite diffusion) and a series combination of resistor and a constant phase element (which is used to model non-ideal capacitive behavior) (12).

It is interesting to compare the values for ΔC calculated from impedance and cyclic voltammetric data, since they should be identical. For systems where there is little interaction between the redox centers (e.g., ferri/ferrocyanide in poly [vinylpyridine] [7]), there is good agreement between the data from the two experiments. If there is some

interaction between centers, then, for some systems (e.g., osmium bipyridine complexes covalently bound to poly [vinylpyridine] [8]), good agreement is again possible if a factor is included in the calculations to account for these interactions. However, for other systems (e.g., iridium hexachloride in poly [vinylpyridine] [7]), there is good agreement when the concentration of redox centers is low, but poor agreement at higher concentrations. The reasons for this behavior are not yet fully understood (13).

To summarize the above discussion, there are two important parameters that define the properties of redox polymers—the diffusion coefficient for electron transfer, and the redox capacitance (charge storage ability) of the film. These can be measured using DC techniques (cyclic voltammetry and chronocoulometry), but there can be some advantage to measuring these parameters using electrochemical impedance spectroscopy, since values for both parameters can be extracted from one experiment. These two parameters can have important practi-

cal applications. For example, the ability of a given redox polymer to act as mediator for an enzyme-based biosensor can be determined by the rate at which the activity of the active site is restored by electron transfer. The energy storage capabilities (which are related to their charge storage capabilities) of redox polymer films are also of considerable interest.

References

1. R.W. Murray, *Electroanalytical Chemistry*; A.J. Bard, ed., Dekker, New York, (1984); Vol. 13, p. 191.
2. H.D. Abruna, *Coord. Chem. Rev.* 86 (1988) 135.
3. M.E.G. Lyons, *Electroactive Polymer Electrochemistry, Part I: Fundamentals*; Plenum Press, New York, (1994).
4. A.W. Bott, *Curr. Seps.* 17 (1998) 25 and references therein.
5. G. Inzelt, *Electroanalytical Chemistry*; A.J. Bard, ed., Dekker, New York (1994); Vol. 18, p. 89.
6. H. Larsson, B. Lindholm, and M. Sharp, *J. Electroanal. Chem.* 336 (1992) 263.
7. B. Lindholm, *J. Electroanal. Chem.* 289 (1990) 85.
8. H. Larsson and M. Sharp, *J. Electroanal. Chem.* 381 (1995) 133 and references therein.
9. A.W. Bott, *Curr. Seps.* 11 (1992) 61.
10. T.B. Hunter, P.S. Tyler, W.H. Smyrl, and H.S. White, *J. Electrochem. Soc.* 134 (1987) 2198.
11. J. Bisquert, G. Garcia-Belmonte, P. Bueno, E. Longo, and L.O.S. Bulhões, *J. Electroanal. Chem.* 452 (1998) 229.
12. P. Ferloni, M. Mastragostino, and L. Meneghello, *Electrochim. Acta* 41 (1996) 27.
13. B. Lindholm-Sethson, T. Tjärnhage, and M. Sharp, *Electrochim. Acta* 40 (1995) 1675.